

Snake Graphs and Frieze Patterns from Orbifolds

Esther Banaian and Elizabeth Kelley

Department of Mathematics, University of Minnesota, Minneapolis, 55455 USA

Abstract. We give an explicit combinatorial formula for the Laurent expansion of any cluster variable of any generalized cluster algebra from a triangulated orbifold, with respect to any initial seed, and associate frieze patterns to orbifolds.

Keywords: orbifold, generalized cluster algebras, snake graphs, frieze

1 Introduction

Our main result is [Theorem 2](#), a definition of snake graphs from orbifolds that gives combinatorial formulas for the Laurent expansions of cluster variables, with respect to any initial seed, for generalized cluster algebras from orbifolds. In [Propositions 1](#) and [2](#), we extend this definition to closed curves and generalized arcs, respectively. This construction also allows us to associate frieze patterns to orbifolds. [Propositions 3](#) and [4](#) give some properties of these frieze patterns. This work is motivated by, but does not use, unpublished work of Gleitz and Musiker [\[9\]](#).

2 Chekhov-Shapiro Algebras

In 2014, Chekhov and Shapiro defined an extension of ordinary cluster algebras [\[8\]](#) without the restriction that exchange polynomials be strictly binomial [\[3\]](#). Often known as “generalized cluster algebras”, we refer to these as *Chekhov-Shapiro algebras* or simply *CS algebras*. The motivation for introducing these algebras came from a desire to extend existing work on the Teichmüller spaces of Riemann surfaces with holes and orbifold points of order two and three to the more general case of Riemann surfaces with holes and orbifold points of arbitrary order [\[2\]](#).

For a fixed semifield (P, \oplus, \cdot) , let \mathcal{F} be isomorphic to $\mathbb{Q}\mathbb{P}[x_1, \dots, x_n]$.

Definition 1. A generalized labeled seed in \mathcal{F} is a quadruple $(\mathbf{x}, \mathbf{y}, B, \mathbf{Z})$ where $\mathbf{x} = (x_1, \dots, x_n)$ is a free generating set for \mathcal{F} , $\mathbf{y} = (y_1, \dots, y_n)$ is an n -tuple with elements in \mathbb{P} , $B = (b_{ij})$ is a skew-symmetrizable $n \times n$ integer matrix, and $\mathbf{Z} = (z_1, \dots, z_n)$ is a tuple of exchange polynomials. We refer to \mathbf{x} as the cluster of $(\mathbf{x}, \mathbf{y}, B)$, \mathbf{y} as the coefficient tuple, and B as the exchange matrix. The elements x_1, \dots, x_n are the cluster variables of $(\mathbf{x}, \mathbf{y}, B)$ and y_1, \dots, y_n are its coefficient variables.

Mutation in direction k reverses the order of coefficients in the exchange polynomial z_k and does not modify the other exchange relations. When all elements of \mathbf{Z} are binomials, generalized mutation coincides with ordinary mutation.

Definition 2. Let \mathbb{T}_n be the n -regular tree graph, where each vertex has adjacent edges labeled by $\{1, \dots, n\}$. A generalized cluster pattern is a map $\chi : v \rightarrow \Sigma_v$ that sends each vertex v of \mathbb{T}_n to a labeled generalized seed $\Sigma_v = (\mathbf{x}_v, \mathbf{y}_v, B_v, \mathbf{Z})$, such that $\Sigma_{v'} = \mu_k \Sigma_v$ if and only if \mathbb{T}_n contains an edge labeled k between $\Sigma_{v'}$ and Σ_v . The generalized cluster algebra associated with χ is defined as $\mathcal{A}(\chi) = \mathbb{Z}\mathbb{P}[x : x \in \bigcup_v \mathbf{x}_v]$ where $\{x : x \in \bigcup_v \mathbf{x}_v\}$ is the set of all cluster variables appearing in seeds that are (generalized-)mutation-equivalent to Σ_v .

Chekhov and Shapiro proved that their algebras exhibit the Laurent Phenomenon - i.e., the cluster variables can be expressed in terms of any cluster as a Laurent polynomial with non-negative coefficients. They also prove positivity for a subclass of their algebras from orbifolds; here, we offer an explicit combinatorial proof for the same subclass.

3 Cluster Algebras from Orbifolds

An orbifold is a generalization of a manifold where the local structure is given by quotients of open subsets of \mathbb{R}^n under finite group actions. In parallel with the classification of cluster algebras associated with triangulated surfaces [6, 7], Felikson, Shapiro, and Turaev established both a notion of triangulating orbifolds and a classification of cluster algebras from orbifolds [4]. In this section, we briefly review some nomenclature and definitions for triangulations of orbifolds that will be used in later sections. For more details and many examples, we refer the reader to the original paper [4].

Definition 3. An orbifold \mathcal{O} is a triple (S, M, Q) , where S is a bordered surface, M is a finite set of marked points, and Q is a finite set of orbifold points, such that: no point is both a marked point and an orbifold point (i.e., $M \cap Q = \emptyset$); all orbifold points are interior points of S ; and each boundary component of S contains at least one marked point. For notational convenience, $\partial\mathcal{O}$ is often used to refer to ∂S .

Each orbifold point has an associated order. Unlike in [5] where all orbifold points are order 2 or $\frac{1}{2}$, our orbifold points are associated with positive integer orders, $p \geq 2$.

Definition 4. An arc γ on an orbifold $\mathcal{O} = (S, M, Q)$ is a non-self-intersecting curve in S with endpoints in M that is otherwise disjoint from M , Q , and $\partial\mathcal{O}$. Curves that are contractible onto $\partial\mathcal{O}$ are not considered arcs. Arcs are considered up to isotopy class. An arc which cuts out an unpunctured monogon with exactly one point in Q is called a pending arc (sometimes drawn as an arc between the marked and orbifold points), while all other arcs are called ordinary arcs.

We will also consider *generalized arcs*, which have the same restrictions except are allowed self-intersections.

Definition 5. Two arcs are considered compatible if their isotopy classes contain non-intersecting representatives. A triangulation is a maximal collection of pairwise compatible arcs.

Although our ultimate goal is to construct snake graphs directly from the triangulated orbifold rather than lifting to some cover, our proof requires considering a particular covering space [3, 11] of an orbifold with a single orbifold point of order p :

Definition 6. Let Σ_n be an $(n + 1)$ -gon containing one orbifold point of order p with vertices labeled v_1, \dots, v_{n+1} in counterclockwise order, $\tilde{\Sigma}_n$ be a regular $p(n + 1)$ -gon with vertices labeled $v_1, v_2, \dots, v_{p(n+1)}$ in counterclockwise order, and T be a triangulation of Σ_n . The triangulation \tilde{T} is constructed via the following procedure:

- For arcs in T with endpoints $v_i \neq v_j$, add the p arcs in \tilde{T} with endpoints $v_{i+k(n+1)}$ and $v_{j+k(n+1)}$, with $k \in [p - 1]$. For loops based at v_i , add arcs from $v_{i+k(n+1)}$ to $v_{i+(k+1)(n+1)}$.
- If $p > 3$, \tilde{T} will still have a central p -gon that hasn't been fully triangulated. Denote the vertices of this central polygon as w_1, \dots, w_p and add arcs with endpoints w_i and w_{i+2} (modulo p). A complete triangulation can be obtained by iteratively repeating this step until the central polygon has been reduced to a triangle.

We refer to $\tilde{\Sigma}_n$ as either the \mathbb{Z}_p -orbit space of $\tilde{\Sigma}_n$ or the p -fold covering.

An example of the 3-fold and 4-fold coverings for a triangle with a single orbifold point are shown in Figure 1. Note that for all $k \in [p - 1]$, restricting \tilde{T} to the vertex set $\{v_{1+k(n+1)}, \dots, v_{(n+1)+k(n+1)}\}$, restoring the orbifold point, and then identifying $v_{i+k(n+1)}$ and $v_{(n+1)+k(n+1)}$ yields a copy of T .

The case of cluster algebras from surfaces (in our notation, $Q = \emptyset$) is well studied. The correspondence between surfaces and cluster algebras is established by Fomin-Thurston.

Theorem 1 (Fomin-Thurston [7]). *Given a surface with marked points, (S, M) , there exists a unique cluster algebra $\mathcal{A} = \mathcal{A}(S, M)$ with the following properties: (1) the seeds are in bijection with tagged triangulations of (S, M) ; (2) the cluster variables are in bijection with tagged arcs in (S, M) ; and (3) the cluster variable x_γ corresponding to arc γ is given by the lambda length of γ , in terms of some initial triangulation.*

In this dictionary, mutation of cluster variables in \mathcal{A} is equivalent to flipping arcs in the triangulation T . An arc τ in T acts locally as a diagonal in a quadrilateral. Thus, the result of flipping τ in T is a new triangulation, $T' = (T - \{\tau\}) \cup \{\tau'\}$ where τ' is the other diagonal of the quadrilateral surrounding τ .

In [3], Chekhov and Shapiro show that flipping pending arcs induces a trinomial exchange relation, which allows them to give an algebraic structure to the dynamics of arcs on orbifolds. We set λ_p to be $2 \cos(\pi/p)$.

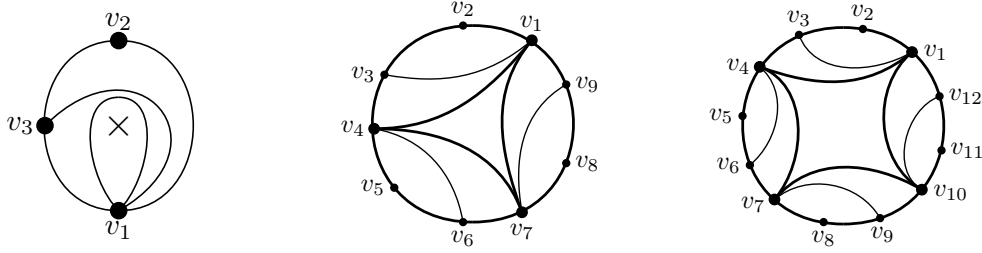


Figure 1: An example of a triangulated orbifold with a single orbifold point of order p (left) and the covering spaces for $p = 3$ (middle) and $p = 4$ (right).

Lemma 1 (Chekhov-Shapiro [3]). *Theorem 1* also holds for an orbifold \mathcal{O} where $\mathcal{A}(\mathcal{O})$ is a CS algebra, with all exchange polynomials being either $z_i(u) = u + 1$ (for ordinary arcs) or $z_i(u) = u^2 + \lambda_p u + 1$ (for pending arcs incident to orbifold points of order p).

4 Snake Graphs

Let $T = \{\tau_1, \dots, \tau_n\}$ be a triangulation of \mathcal{O} . Let $\{\tau_{n+1}, \dots, \tau_c\}$ be the boundary arcs of \mathcal{O} . For now, we work with orbifolds without any punctures, but we expect our results to hold when we introduce punctures.

Given an arbitrary arc γ on \mathcal{O} with triangulation T , we can use the Ptolemy relation to write γ as a rational function in terms of $\{\tau_1, \dots, \tau_c\}$. However, determining an expansion via this method can be computationally challenging. To simplify this process, we generalize the snake graph construction due to Musiker, Schiffler, and Williams [13], obtaining a combinatorial formula for the expansion in terms of the perfect matchings of a particular weighted graph, called a *snake graph*.

Fix an arbitrary triangulation T of \mathcal{O} and arc γ (either ordinary, pending, or generalized). We recursively construct the snake graph $G_{T,\gamma}$ by gluing together square *tiles* determined by the intersections of γ with arcs of T . Further, if γ is a closed curve, we can similarly construct a band graph.

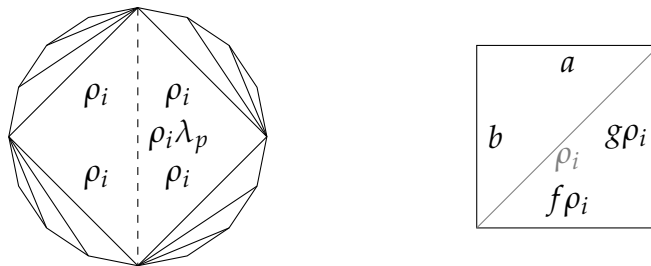
4.1 Tiles

If $\gamma = \tau_i$ for $1 \leq i \leq n$ (recall the final $c - n$ arcs are boundary arcs), then G_γ is a single edge labeled with τ_i . Otherwise, choose some orientation for γ . Since T is a maximal set of non-intersecting arcs, in this case γ will cross at least one arc in T .

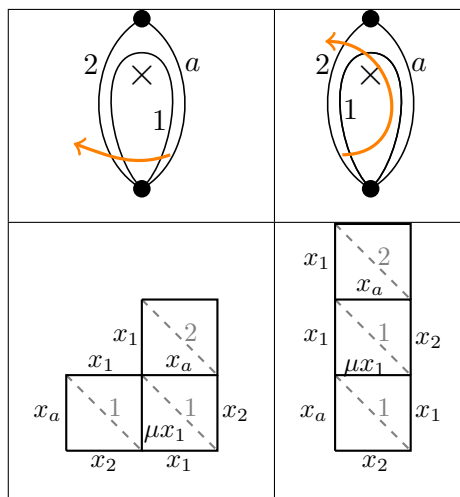
Let ρ_1, \dots, ρ_m be the set of internal arcs of T that γ crosses, given a fixed orientation. For each ordinary arc ρ_i that γ crosses, we construct a square tile G_i by taking the two triangles that ρ borders and gluing them along ρ , such that either both have either the same or opposite orientation as in \mathcal{O} . We say that the former case has relative orientation $+1$ and the latter case has relative orientation -1 , denoted as $\text{rel}(G_i) = \pm 1$.



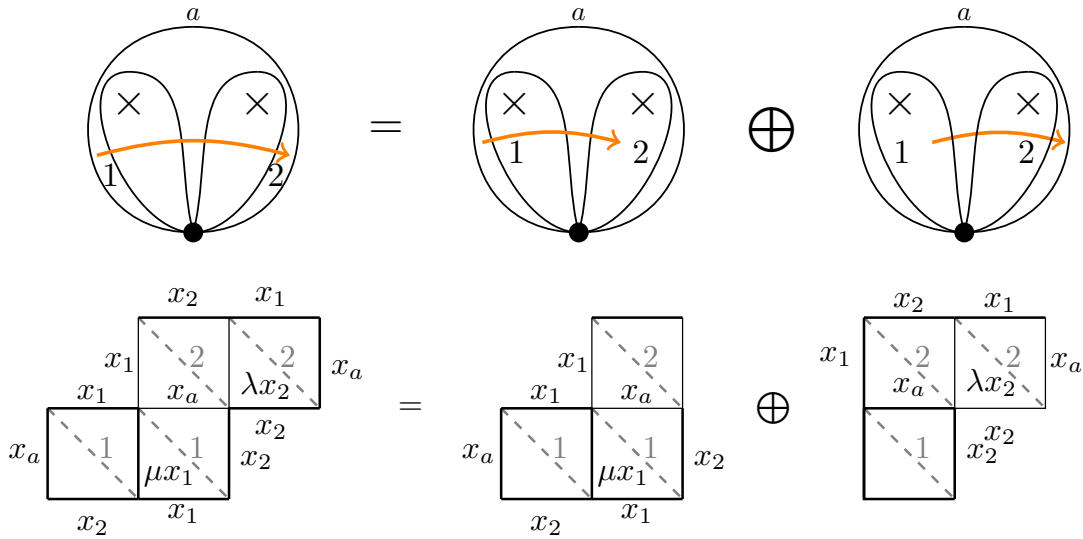
If ρ_i is a pending arc encircling an orbifold point of order p , then it is only incident to one triangle in \mathcal{O} . As inspiration for the other triangle, we look to the p -fold cover around this orbifold point. For $p > 3$, this surface is not triangulated since we have a central ideal p -gon. However, for a regular p -gon, with each side length ρ_i , the length of the diagonal that bypasses exactly one vertex (a "2-diagonal") is $\frac{\sin(2\pi/p)}{\sin(\pi/p)}\rho_i = 2 \cos(\pi/p)\rho_i$. Recall this is the same parameter that appears when we mutate pending arcs. We use this 2-diagonal in the p -fold cover as an auxiliary arc to define a second triangle that ρ_i borders, as on the left hand side below.



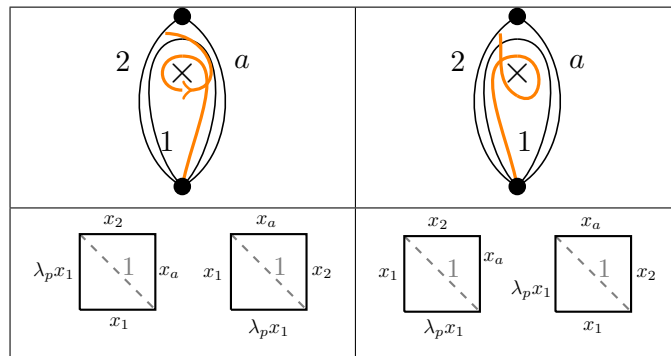
On the right, $\{f, g\} = \{1, \lambda_p\}$ as sets. We define the orientation of the tile based on whether the orientation of the triangle with edges a, b, ρ_i matches or does not match that on the surface. We determine f and g by the relative orientation of γ 's path, as below.



The other labels of the tile labeled 2 will depend on the local configuration around 2. In the configurations above, 2 could be either ordinary arc or a pending arc. If 2 is a pending arc, then we would need to use such a configuration twice. We use one configuration for both crossings of 1 and one crossing of 2, and the second for one crossing of 1 and both crossings of 2. Below is one example of such gluing - we could do something similar if γ matched the orientation in the right hand diagram.



In the case of ordinary arcs, crossing a pending arc produces two square tiles since it involves two actual crossings. When constructing the snake graph for a generalized arc γ , however, it's possible to have only one crossing. In this case, the following rules are used to determine f and g :



4.2 Gluing $G_{T,\gamma}$

We then glue these square tiles together, according to the following rule: when crossing two consecutive arcs τ_i and τ_{i+1} , we glue G_i and G_{i+1} along the shared edge labeled $\tau_{[i]}$,

using the appropriate planar embeddings so $\text{rel}(T, G_i) \neq \text{rel}(T, G_{i+1})$. Note that this rule does not differentiate between ordinary and pending arcs.

Because the choice of relative orientation for the first tile, G_1 , isn't fixed, there are two valid planar embeddings of $G_{T,\gamma}$ for any γ . Our cluster expansion formula produces the same result for either choice of planar embedding, so the choice is unimportant.

Finally, we can construct generalized band graphs using the same ideas. Band graphs calculate the length of closed curves in a surface. Choose a point p on γ such that p does not lie on any arc in T or at an intersection of γ with itself. For simplicity, we require p to not be in the interior of a pending arc. Then, construct the snake graph for γ , picking an orientation and starting and ending at p . Since the first and last tile correspond to arcs bordering the same triangle, they will have a common edge. We glue the first and tile along this edge. This gives a graph which resembles an annulus or a Mobius strip. Statistics associated to a band graph are the same as for snake graphs

4.3 Cluster Expansion Formulas

To state the cluster expansion formula, we need the following definition:

Definition 7 ([13]). *Each snake graph has exactly two perfect matchings which use only boundary edges. One of these matchings uses the south edge of the first tile and the other uses the west edge of the first tile. By convention, we refer to the boundary matching which uses the west edge as the minimal matching, P_- , of P .*

For an arbitrary perfect matching P of $G_{T,\gamma}$, we sometimes consider the symmetric difference $P \ominus P_-$. For all P , this symmetric difference consists of a set of potentially disjoint cycles. We now define some statistics associated to γ and $G_{T,\gamma}$, following [13]:

- The *crossing monomial* is $\text{cross}(T, \gamma) = \prod_{\tau_i \in T} x_i^{e(x_i, \gamma)}$, where $e(x_i, \gamma)$ is the minimal number of crossings of γ with arcs in the isotopy class of τ_i .
- The *weight* $x(P)$ of a perfect matching P of $G_{T,\gamma}$ is the product of all its edge weights - i.e., if the edges of P has labels $\tau_{i_1}, \dots, \tau_{i_k}$, then $x(P) = x_{\tau_{i_1}} \cdots x_{\tau_{i_k}}$.
- The *height monomial* $y(P)$ is $y(P) = \prod_{\tau_i \in T} y_i^{m_i}$, where m_i is the multiplicity of tiles labeled i enclosed by cycles of $P \ominus P_-$.

We are then able to establish the following theorem for Laurent expansions of arcs (both ordinary and pending), a slightly more general version of the theorem from [13].

Theorem 2. *Let $\mathcal{O} = (S, M, Q)$ be an arbitrary orbifold with triangulation T and \mathcal{A} be the corresponding CS algebra with principal coefficients with respect to $\Sigma_T = (\mathbf{x}_T, \mathbf{y}_T, B_T)$. For an arc γ with snake graph $G_{T,\gamma}$, the Laurent expansion of x_γ with respect to Σ_T is*

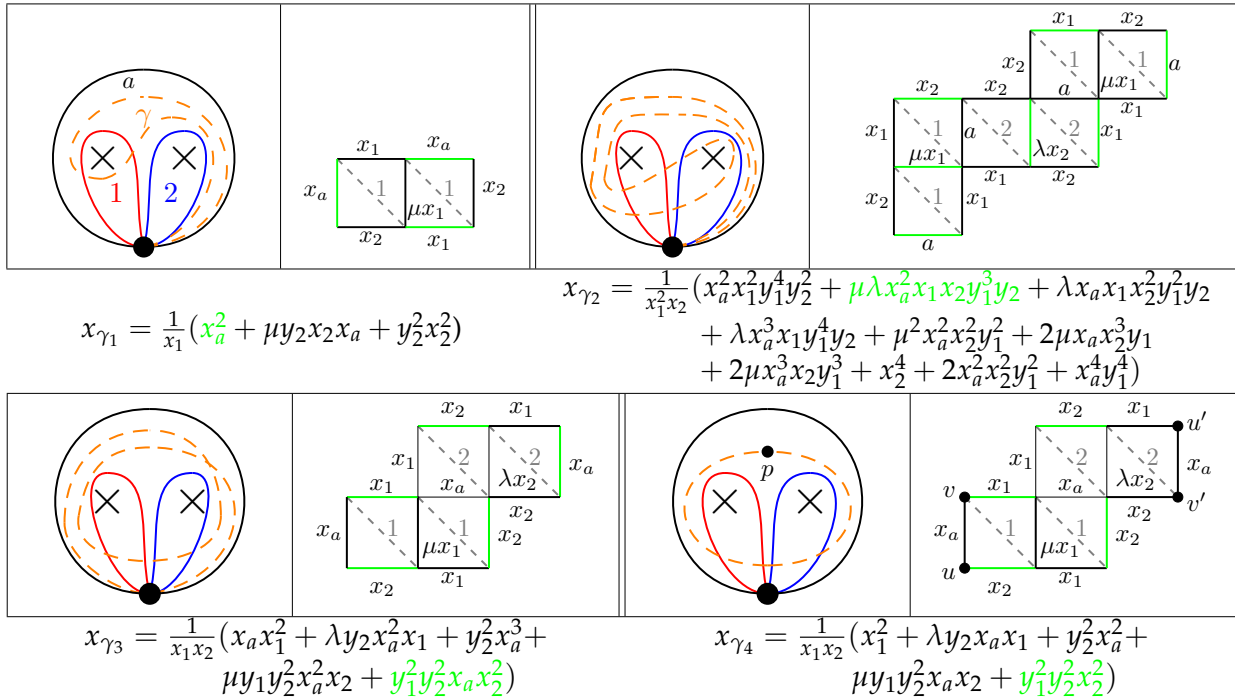
$$[x_\gamma]_{\Sigma_T}^{\mathcal{A}} = \frac{1}{\text{cross}(T^\circ, \gamma)} \sum_P x(P)y(P)$$

where the summation is indexed by perfect matchings of $G_{T,\gamma}$.

Proposition 1. Let γ be a generalized arc in \mathcal{O} . If γ has a contractible kink, let γ' be the same curve with the kink removed. Then, $x_\gamma = (-1)x_{\gamma'}$. Otherwise, $x_\gamma = \frac{1}{\text{cross}(T^\circ, \gamma)} \sum_P x(P)y(P)$ where the summation is indexed by perfect matchings of $G_{T,\gamma}$.

Proposition 2. Let γ be a closed curve on \mathcal{O} . If γ is contractible, then $x_\gamma = -2$. Otherwise, [Theorem 2](#) also holds where $G_{T,\gamma}$ is a generalized band graph.

Example 1. The table below shows snake graphs for a variety of curves on the triangulated orbifold corresponding to $\mathcal{A} = \left(\mathbf{x}, \mathbf{y}, \begin{bmatrix} 0 & -1 \\ 1 & 0 \end{bmatrix}, (1 + \mu u + u^2, 1 + \lambda u + u^2) \right)$.



Labels for arcs in the initial triangulation are only shown in the first orbifold diagram, but are consistent throughout. Snake graphs are shown for each (dashed) curve γ_i , with one perfect matching (and the corresponding term in the Laurent expansion) highlighted. Both γ_1 and γ_2 are cluster variables of \mathcal{A} , obtained via the respective mutation sequences μ_1 and $\mu_2 \mu_1$.

The second half of this example illustrates the extension of our results to generalized arcs and closed curves. Since γ_3 and γ_4 cross the same arcs in the same orientation, the shapes of the two associated graphs are the same. However, in the band graph associated to γ_4 , we identify u with u' and v with v' . In each of these graphs, we have highlighted the maximal matching.

Note that in each of these examples, our expression for x_{γ_i} is given after canceling a mutual factor from the crossing monomial and the numerator. Although the exact mutual factor depends on the curve being considered, cancellation of this type occurs whenever we cross pending arcs.

5 Frieze Patterns

Periodic frieze patterns of positive integers have been shown to be in bijection with triangulated surfaces; those with a finite number of rows correspond to triangulated polygons, while those with infinitely many rows correspond to triangulations of annuli.

Holm and Jørgensen classified a certain family of finite frieze patterns associated with *polygon dissections* [10]. A polygon dissection is a generalization of a triangulation, in the sense that it is a (not necessarily maximal) set of pairwise non-intersecting arcs on a surface. The entries in these frieze patterns are positive integer combinations of λ_p for finitely many values of p . Our snake graphs from orbifolds allow us to construct infinite frieze patterns in the spirit of Holm and Jørgensen and to recover some of their finite frieze patterns.

Definition 8. A (finite) frieze pattern is a (finite) set of infinite rows, where each row is offset from its neighbors in such a way that the entries of every other row form columns. The first row consists of all zeroes and the second row consists of all ones. The defining property of a frieze

pattern is that every diamond $\begin{array}{c} a \\ b \quad c \\ d \end{array}$ satisfies the condition $bc - ad = 1$.

Note that once we specify the first nontrivial row, the entire frieze pattern is determined. We refer to this first nontrivial row as the *quiddity row*.

We use the following indexing to refer to entries of a frieze pattern. We can also refer to entries in the row of 0's as (i, i) and in the row of 1's as $(i, i + 1)$.

$$\begin{array}{cccccccc} 0 & & 0 & & 0 & & 0 & & 0 \\ & 1 & & 1 & & 1 & & 1 & & 1 \\ (1,3) & & (2,4) & & (3,5) & & (4,6) & & (5,7) \\ & (1,4) & & (2,5) & & (3,6) & & (4,7) & & (5,8) \\ (0,4) & & (1,5) & & (2,6) & & (3,7) & & (4,8) \\ & (0,5) & & (1,6) & & (2,7) & & (3,8) & & (4,9) \\ & & & & & \vdots & & & & \end{array}$$

While there are several combinatorial interpretations of entries in frieze patterns of positive integers, we can also interpret each entry as giving the length of an arc on the triangulated surface corresponding to the frieze pattern. In this interpretation, the

length of all boundary arcs and arcs in the triangulation is set to 1. In a finite frieze pattern associated to a triangulation of an n -gon, entry (i, j) corresponds to the length of the diagonal between vertices \bar{i} and \bar{j} where $\bar{i} \equiv i \pmod{n}$. There is a similar story for infinite frieze patterns, except we must keep track of how many times an arc winds around the annulus. Moreover, the frieze pattern only measures *peripheral arcs* along the outer boundary (although we could also make a frieze pattern with respect to the inner boundary). A peripheral arc is the result of concatenating multiple boundary arcs from the same boundary. In a polygon, all arcs are peripheral. The following Lemma is part of a larger theorem in [12], and holds for more general surfaces than discussed there.

Lemma 2. *A frieze pattern corresponding to a triangulated surface encodes a map on peripheral arcs on the surface which respects the Ptolemy relation.*

Our snake graphs allow us to measure the length of arcs in a triangulated orbifold in terms of the lengths of the arcs in the triangulation. We set all of these lengths to 1; however, we could also recover a frieze pattern of Laurent polynomials by leaving the lengths as variables.

We construct $\mathcal{F}(\mathcal{O})$, a frieze pattern associated to a triangulated orbifold, \mathcal{O} . We distinguish one boundary to work with respect to.

- Let $\gamma_1, \dots, \gamma_m$ be the set of peripheral arcs along one boundary component which are the result of concatenating exactly two boundary arcs.
- Let $X(\gamma_i)$ be the sum of perfect matchings of G_{γ_i} with all $x_j = y_j = 1$.
- The frieze pattern $\mathcal{F}(\mathcal{O})$ is determined by a quiddity row given by repeating $X(\gamma_1), X(\gamma_2), \dots, X(\gamma_m)$ infinitely many times.

By **Lemma 1**, we know that an orbifold surface \mathcal{O} encodes a CS algebra \mathcal{A} , so some cluster variables and other elements of \mathcal{A} are lambda lengths of arcs on \mathcal{O} . By **Theorem 2** and **Proposition 1**, we can express these elements of \mathcal{A} in terms of perfect matchings. This implies the following interpretation of these frieze patterns:

Proposition 3. *The entries in $\mathcal{F}(\mathcal{O})$ are specializations of elements of $\mathcal{A}(\mathcal{O})$, where we set all initial variables x_i and y_i to 1.*

Because our edge weights are all positive, we also observe that:

Corollary 1. *If p_1, \dots, p_k are the orders of the orbifold points in \mathcal{O} , then all entries of $\mathcal{F}(\mathcal{O})$ are positive integer multiples of $1, \lambda_{p_1}, \dots, \lambda_{p_k}$.*

Our earlier example illustrates that, in the case of an orbifold with two orbifold points, we can have arcs which wind around the two points arbitrarily many times. The same is true for a surface with multiple boundary components, such as an annulus, or a surface with punctures. This leads us to the following.

Proposition 4. *The frieze pattern $\mathcal{F}(\mathcal{O})$ is finite if and only if S is homeomorphic to a disk, $|Q| = 1$ and $M \cap \partial S = M$. In particular, if S has n marked points on the boundary and the unique orbifold point is order p , then $\mathcal{F}(\mathcal{O})$ has $np - 3$ nontrivial rows.*

Note that the orbifolds which give finite frieze patterns are exactly those whose cover is an unpunctured polygon. The triangulation of the orbifold lifts to a polygon dissection of the cover. In these cases, the frieze pattern we construct from the orbifold matches the frieze pattern Holm and Jørgensen associate with the cover. This is the case for the left hand frieze below, which is the frieze pattern associated to the orbifold in [Figure 1](#) where the orbifold point has order 4 ($\lambda_4 = \sqrt{2}$). This frieze pattern is 3-periodic and by [Proposition 4](#) we know it has 9 nontrivial rows.

$$\begin{array}{cccccccc} 0 & & 0 & & 0 & & 0 & \\ & 1 & & & 1 & & 1 & \\ 1 & & 2 & & 3 + \sqrt{2} & & 1 & \\ & 1 & & & 5 + 2\sqrt{2} & & 2 + \sqrt{2} & \\ 1 + \sqrt{2} & 2 + \sqrt{2} & & & 3 + 2\sqrt{2} & & 1 + \sqrt{2} & \end{array} \parallel \begin{array}{ccc} & 0 & \\ 1 & & 1 \\ & 3 + 2\sqrt{2} & \\ 16 + 12\sqrt{2} & & 16 + 12\sqrt{2} \\ & 93 + 66\sqrt{2} & \end{array}$$

The right hand frieze is associated to the orbifold in [Example 1](#), with both orbifold points again order 4. Since this orbifold has two orbifold points, we know that there are infinitely many rows. This frieze pattern is 1-periodic, with the quiddity row determined by the bottom left arc in [Example 1](#), which is the concatenation of arc a with itself.

Meanwhile, [\[1\]](#) demonstrated a set of invariants for periodic, infinite frieze patterns. Given an infinite frieze pattern \mathcal{F} , let n be the minimal period of the quiddity row. Then, using our indexing above and fixing $k \geq 1$, the difference $(j, j + nk + 1) - (j + 1, j + nk - 1)$ is constant for all j . These parameters are referred to as *growth coefficients*. In the case of positive integers, where the frieze patterns arise from triangulations of annuli, [\[12\]](#) gave a geometric interpretation for these growth coefficients. Specifically, they showed that the k -th growth coefficient corresponds to the length of a closed curve which winds around the annulus k times. We conjecture that our generalized band graphs will allow us also to keep track of growth coefficients of the frieze patterns from triangulated orbifolds.

Conjecture 1. *Generalized band graphs determine the growth coefficients of infinite friezes arising from orbifolds.*

As evidence to support our conjecture, observe that the first growth coefficient for the infinite frieze above is $3 + 2\sqrt{2}$, which agrees with x_{γ_4} from [Example 1](#) when the Laurent expansion is evaluated at $x_i = 1$ and $\lambda = \mu = \sqrt{2}$.

References

- [1] K. Baur, K. Fellner, M. J. Parsons, and M. Tschabold. “Growth behaviour of periodic tame friezes”. *Revista Matemática Iberoamericana* 35.2 (2018), pp. 575–606. [Link](#).

- [2] L. Chekhov and M. Mazzocco. “Isomonodromic deformations and twisted Yangians arising in Teichmüller theory”. *Adv. in Math.* **266.6** (2011), pp. 4731–4775. [Link](#).
- [3] L. Chekhov and M. Shapiro. “Teichmüller Spaces of Riemann Surfaces with Orbifold Points of Arbitrary Order and Cluster Variables”. *Int. Math. Res. Not.* **10** (2014), pp. 2746–2772. [Link](#).
- [4] A. Felikson, M. Shapiro, and P. Tumarkin. “Cluster algebras and triangulated orbifolds”. *Adv. in Math.* **231.5** (2012), pp. 2953–3002. [Link](#).
- [5] A. Felikson, M. Shapiro, and P. Tumarkin. “Cluster algebras of finite mutation type via unfoldings”. *Int. Math. Res. Not.* **8** (2012), pp. 1768–1804. [Link](#).
- [6] S. Fomin, M. Shapiro, and D. Thurston. “Cluster algebras and triangulated surfaces. I: Cluster complexes”. *Acta Math.* **201.1** (2008), pp. 83–146. [Link](#).
- [7] S. Fomin and D. Thurston. *Cluster algebras and triangulated surfaces. II: Lambda lengths*. Mem. Amer. Math. Soc 1223. Amer. Math. Soc., Providence, RI, 2012. [Link](#).
- [8] S. Fomin and A. Zelevinsky. “Cluster Algebras I: Foundations”. *J. Amer. Math. Soc.* **15.2** (2002), pp. 497–529. [Link](#).
- [9] A.-S. Gleitz and G. Musiker. Private communication.
- [10] T. Holm and P. Jorgensen. “A p -angulated generalisation of Conway and Coxeter’s theorem on frieze patterns”. *Int. Math. Res. Not.* (2017), rny020. [Link](#).
- [11] D. Labardini-Fragoso and D. Velasco. “On a family of Caldero-Chapoton algebras that have the Laurent Phenomenon”. 2017. [arXiv:1704.07921](#).
- [12] G. Musiker, E. Gunawan, and H. Vogel. “Cluster algebraic interpretation of infinite friezes”. 2016. [arXiv:1611.03052](#).
- [13] G. Musiker, L. Williams, and R. Schiffler. “Positivity for cluster algebras from surfaces”. *Adv. in Math.* **227.6** (2011), pp. 2241–2308. [Link](#).